Science Translational Medicine
AAAS

stm.sciencemag.org/cgi/content/full/12/558/eabc0441/DC1

Supplementary Materials for

Gastrointestinal synthetic epithelial linings

Junwei Li, Thomas Wang, Ameya R. Kirtane, Yunhua Shi, Alexis Jones, Zaina Moussa, Aaron Lopes, Joy Collins, Siddartha M. Tamang, Kaitlyn Hess, Rameen Shakur, Paramesh Karandikar, Jung Seung Lee, Hen-Wei Huang, Alison Hayward, Giovanni Traverso*

*Corresponding author. Email: cgt20@mit.edu, ctraverso@bwh.harvard.edu

Published 26 August 2020, *Sci. Transl. Med.* **12**, eabc0441 (2020)
DOI: 10.1126/scitranslmed.abc0441

The PDF file includes:

Other Supplementary Material for this manuscript includes the following:

(available at stm.sciencemag.org/cgi/content/full/12/558/eabc0441/DC1)

Materials and Methods

Abbreviations:

GSEL: gastrointestinal synthetic epithelial linings; PDA: polydopamine; PBS: phosphate-buffered saline; IgG: immunoglobulin G; FTIR: Fourier transform infrared.

Chemicals and materials:

Dopamine hydrochloride (1225204), simulated gastric fluid (18818), urea H_2O_2 (289132), catalase (C3556 & C1345), Triton X-100 (T8787), 3-amino-1,2,4-triazole (A8056), RIPA buffer (R0278), protease inhibitor cocktail (P8340), phosphatase inhibitor cocktail 3 (P0044), Trizma base, o-nitrophenol-β-D-galactoside (N1127), β-Galactosidase (1356698), glucose (G8270), and lactose (17814) were purchased from Sigma-Aldrich. Formalin (10%, phosphate buffered) (SF100), Tissue-Plus O.C.T (23-730-571), BD GasPak EZ gas generating systems incubation containers (B260002) and SouthernBiotech Fluoromount-G slide mounting medium (OB100) were purchased from Fisher Scientific. Pierce BCA protein assay (23225), Pierce DAB substrate (34002), Pierce 16% formaldehyde (w/v) (28908), rabbit anti-goat immunoglobulin G (IgG) (H+L) secondary antibody-HRP (31402), goat anti-rabbit IgG (H+L) secondary antibody-HRP (65-6120), Vybrant MTT cell viability assay (V13154), Dynabeads M-280 (tosyl activated) (14203), SeeBlue Plus2 pre-stained protein standard (LC5925), SuperSignal West Femto Maximum Sensitivity substrate (34094), Pierce ECL western blotting substrate (32109), NuPAGE 4-12% Bis-Tris protein gels (NP0321BOX), NE-PER nuclear and cytoplasmic extraction kit (78835), Mem-PER plus membrane protein extraction kit (89842), antibiotic-antimycotic (100X) (15240062), SuperScript IV reverse transcriptase (18090050), PCR Master Mix, and all primers were purchased from ThermoFisher. Total RNA isolation kit was purchased from ZYMO RESEARCH. Precision Plus Protein dual color standard (#1610374) was purchased from Bio-Rad. Barium sulfate (13989) was purchased from Alfa Aesar. Simulated intestinal fluid was purchased from VWR. CYP3A4 activity assay kit (ab211076), calcium assay kit (ab102505), glutamate assay kit (ab138883), anti-catalase and anti-β-actin antibodies were purchased from Abcam. Catalase (CAT) assay kit (E-BC-K031) was purchased from Elabscience. Praziquantel was purchased from Ark Pharm. Sieves (150 and 300 μm mesh sizes) were purchased from McMaster-Carr. Glo-Tip spray catheter (G24892) was purchased from COOK Medical. All other chemicals and bio-chemicals (unless specified) were purchased from Sigma-Aldrich and used without further purification.

Tissue lysate preparation. Epithelial tissues of the porcine gastrointestinal tract were dissected on ice. The outer mucus layers were removed by aspiration, and then the rinsed tissues [(with 1X phosphate-buffered saline (PBS)] were frozen by liquid nitrogen. Tissues (10 mg) were incubated in the ice-cold lysis buffer (600 μl, RIPA buffer mixed with protease and phosphatase inhibitor cocktail, Sigma-Aldrich) and homogenized to form tissue lysates. The total protein concentrations of tissue lysates were measured by using the bicinchoninic acid (BCA) assay.

Catalytic capacity analysis of tissue lysates. A native gel-based catalytic activity assay was performed. Proteins in tissue lysates were resolved on a 7.5**%** non-denaturing polyacrylamide gel, and the gel was stained by the gastrointestinal synthetic epithelial linings (GSEL) solution (50 ml) for 10 minutes. After staining, the gel was washed 3 times with PBS buffer (1X) and imaged.

In vitro inhibition of CAT activity in tissue lysates. The inhibition of CAT activity was performed as previously reported*(64)*. 3-amino-1,2,4-triazole was used as the inhibitor. Tissue lysates (10 mg/ml, 100 μl) were incubated in the inhibitor solution (20 mM) for 6 hours at 4 °C.

Immunoprecipitation of CAT in tissue lysates. CAT antibody was first conjugated on tosyl-activated magnetic beads (Dynabeads M-280) based on the Dynabeads protocol. The conjugated beads (60 mg) were further added into tissue lysate solutions (10 mg/ml, 100 μl), incubated for 2 hours to capture CAT in the solutions, and placed on the magnet for 2 minutes to remove beads.

Serum praziquantel concentration assessment. Praziquantel concentrations in serum from in vivo experiments were analyzed using Ultra-Performance Liquid Chromatography-Tandem Mass Spectrometry (UPLC-MS/MS). Analysis was performed on a Waters ACQUITY UPLC-I-Class System aligned with a Waters Xevo TQ-S mass spectrometer (Waters Corporation, Milford MA). Liquid chromatographic separation was performed on an Acquity UPLC BEH C18 (50 mm × 2.1 mm, 1.7-μm particle size) column at 50 °C. The mobile phase consisted of aqueous 0.1% formic acid, 10 mM ammonium formate solution (Mobile Phase A) and acetonitrile: 10 mM ammonium formate, 0.1% formic acid solution (95:5 v/v) (Mobile Phase B). The mobile phase had a continuous flow rate of 0.6 ml/min using a time and solvent gradient composition. For the analysis of praziquantel, the initial composition, 80% Mobile Phase A, was held for 0.50 minutes, following which the composition was changed linearly to 0% Mobile Phase A over the next 2.00 minutes. The composition of 0% Mobile Phase A and 100% Mobile Phase B was held constant until 3.50 minutes. The composition returned to 80% Mobile Phase A at 3.51 minutes and was held at this composition until completion of the run, ending at 5.00 minutes, where it remained for column equilibration. The total run time was 5.00 minutes. The mass to charge transitions (m/z) used to quantitate praziquantel were 313.22>203.09 and 313.22>83.01 for quantitation and confirmation respectively. As an internal standard, mebendazole, 296.06>264.03 and 296.06>76.99 m/z transitions were used for quantitation and confirmation respectively. Sample introduction and ionization was by electrospray ionization (ESI) in the positive ionization mode. Waters MassLynx 4.1 software was

used for data acquisition and analysis. Stock solutions of praziquantel were prepared in methanol at a concentration of 500 µg/ml. A twelve-point calibration curve was prepared in analyte-free, blank serum ranging from 1.25-5000 ng/ml. 100 µl of each serum sample was spiked with 200 µl of 250 ng/ml mebendazole in acetonitrile to elicit protein precipitation. Samples were vortexed, sonicated for 10 minutes, and centrifuged for 10 minutes at 13,000 rpm. 200 µl of supernatant was pipetted into a 96-well plate containing 200 µl of water. Finally, 1.00 µl was injected onto the UPLC-ESI-MS system for analysis.

Serum and tissue dopamine concentration assessment. Dopamine concentrations in serum and tissue from in vivo experiments were analyzed using Ultra-Performance Liquid Chromatography-Tandem Mass Spectrometry (UPLC-MS/MS). Analysis was performed on a Waters ACQUITY UPLC-I-Class System aligned with a Waters Xevo TQ-S mass spectrometer (Waters Corporation, Milford MA). Liquid chromatographic separation was performed on an Acquity UPLC BEH C18 (50 mm × 2.1 mm, 1.7-µm particle size) column at 50 °C. The mobile phase consisted of aqueous 0.1% formic acid, 10 mM ammonium formate solution (Mobile Phase A) and acetonitrile: 10 mM ammonium formate, 0.1% formic acid solution (95:5 v/v) (Mobile Phase B). The mobile phase had a continuous flow rate of 0.45 ml/min using a time and solvent gradient composition. Sample introduction and ionization was by electrospray ionization (ESI) in the positive ionization mode. Waters MassLynx 4.1 software was used for data acquisition and analysis. Stock solutions were prepared in methanol at a concentration of 500 µg/ml. A twelve-point calibration curve was prepared in analyte-free, blank porcine serum ranging from 1.25-10000 ng/ml. 100 µl of each serum sample was spiked with 100 µl of 500 ng/ml methyldopamine (internal standard) in acetonitrile to elicit protein precipitation. 200 ul of 5 mg/ml fluorescamine in acetonitrile was then added to each sample as a derivatization agent for both dopamine and methyldopamine to aid in detection. Samples were vortexed, sonicated for 10 minutes, and centrifuged for 10 minutes at 13,000 rpm. 300 µl of supernatant was incubated at 37°C for 60 minutes. 200 ul of incubated solution was then added to 200 ul of water in a 96-well plate. Finally, 10 µl was injected onto the UPLC-ESI-MS system for analysis.

Tissue samples were divided into pieces of about 300 mg. 3% bovine serum albumin in PBS buffer was added at a 2:1 volume to mass ratio. Samples were homogenized at 4°C. 100 µl of each homogenate was spiked with 100 µl of 500 ng/ml methyldopamine in acetonitrile and 200 ul of 5 mg/ml fluorescamine in acetonitrile for derivatization. 1.00 ml of ethyl acetate was added to homogenized samples as well for extraction. Samples were vortexed, sonicated for 10 minutes, and centrifuged for 10 minutes at 13,000 rpm. Following centrifugation, 300 µl of the supernatant was incubated at 37°C for 60 minutes. Samples were allowed to evaporate overnight. The evaporated samples were reconstituted with 300 µl acetonitrile and centrifuged for 5 minutes at 6,000 rpm. 200 µl of the supernatant was pipetted into a 96-well plate containing 200 µl of water. Finally, 10 µl was injected onto the UPLC-ESI-MS system for the analysis.

For the analysis of dopamine fluorescamine, the initial composition, 95% Mobile Phase A, was held for 0.75 minutes. Following which, the composition was changed linearly to 5% Mobile Phase A and 95% Mobile Phase B until 1.00 minute. The composition was held constant at 95% Mobile Phase B until 3.00 minutes. At 3.25 minutes the composition returned to 95% Mobile Phase A, where it remained for column equilibration for the duration of the run, ending at 4.00 minutes. The mass to charge transitions (m/z) used to quantitate dopamine were 414.223>137.125 and 414.223>119.115 for quantitation and confirmation respectively. For internal standard, methyldopamine fluorescamine, 472.223>139.139 and 472.223>278.094 m/z transitions were used for quantitation and confirmation respectively.

Cytotoxicity assay. Vybrant MTT cell proliferation assay was used to test the cytotoxicity of polydopamine (PDA) in living cells. As-prepared PDA was added into the cell culture medium with various concentrations (0, 10, 50, 250, 500, 1000, 1500 and 2000 µg/ml). Cytotoxicity was tested on multiple cell lines: HeLa (ATCC), COLO320DM (ATCC), Caco-2 (ATCC), Hep3B (ATCC), and HS 895.T (ATCC), by seeding them each in a 96-well plate at a density of 10,000 cells, and keeping them in culture for 24 hours before replacing the medium with 100 µl PDA solution. The cells were incubated at 37 °C for various amounts of time (6, 12, 24 hours) in cell culture incubator. The cells were washed 3 times with PBS buffer, followed by addition of the MTT solution (10 µl) and cell culture medium (100 µl) to each well and incubation for 4 hours at 37 °C. After 4 hours, 100 µl SDS-HCl solution was added to each well for another 4 hours incubation (at 37 °C). Absorbance at 570 nm was recorded on a 96-well plate reader (Tecan Infinite M200).

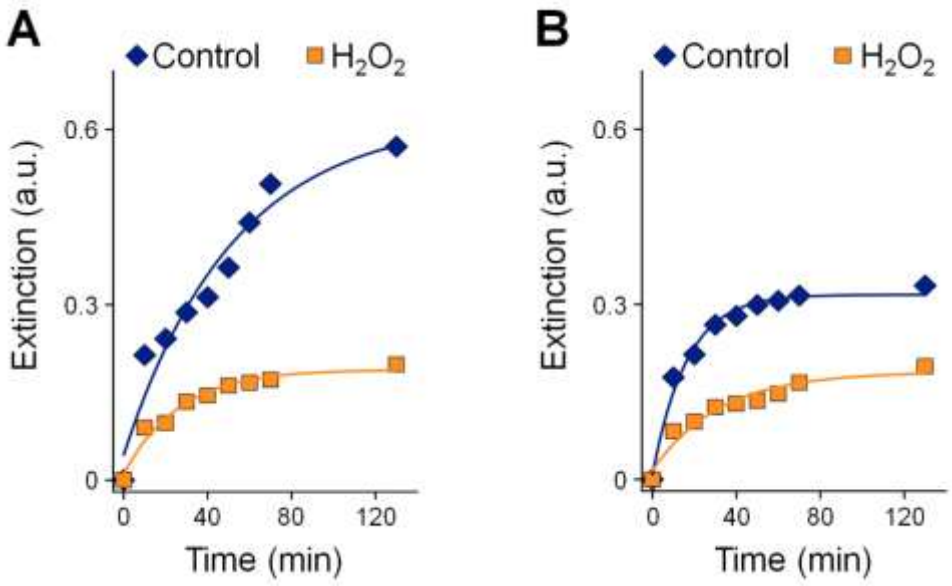

Fig. S1. Comparison of PDA polymerization kinetics under different reaction conditions. (**A**) Extinction measured at 700 nm for the samples [with and without H_2O_2 (control)] undergoing PDA polymerization in the air. (**B**) Extinction measured at 700 nm for the samples [with and without H_2O_2 (control)] undergoing PDA polymerization in extremely low oxygen (hypoxic environment). The addition of H_2O_2 almost quenched the PDA polymerization in the air and in the low oxygen condition.

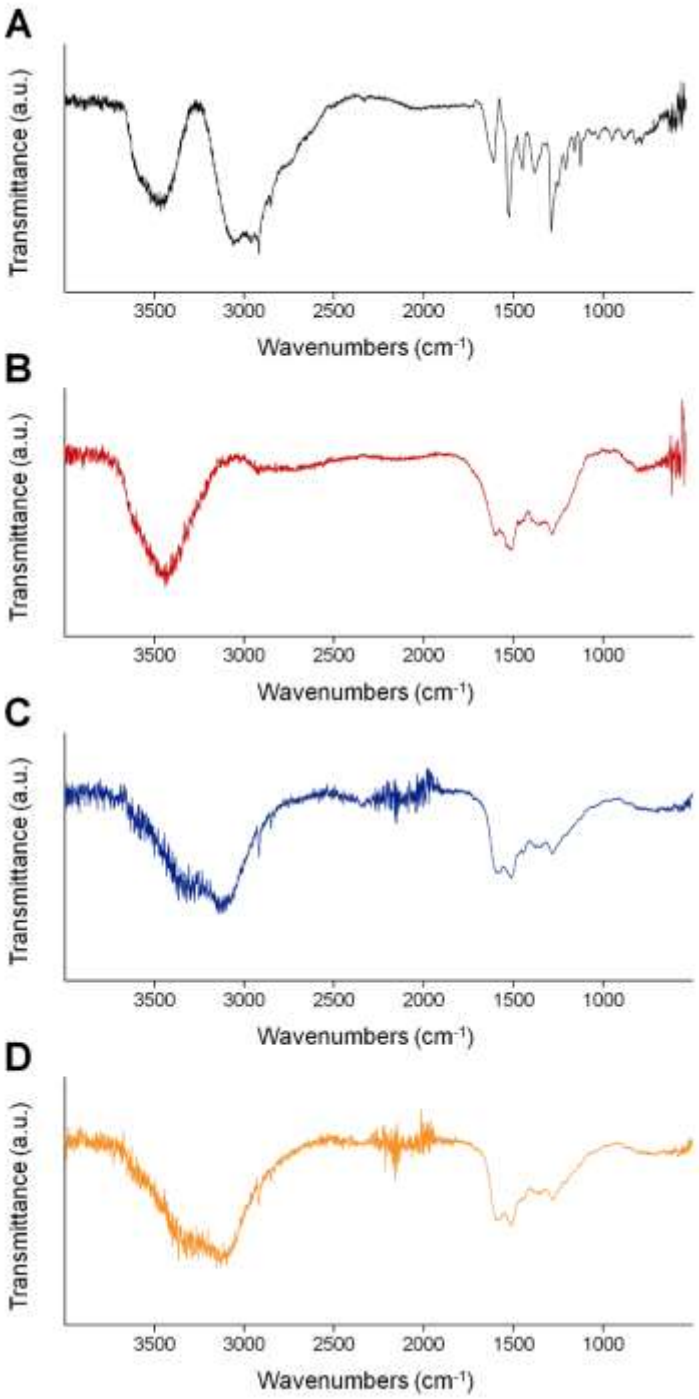

Fig. S2. FTIR spectra of dopamine, PDA standard, and polymerization products. FTIR spectra of (**A**) dopamine and (**B**) PDA prepared under conventional conditions were measured and used as standards. FTIR spectra confirm the PDA formation in the polymerization products under (**C**) CAT (commercially purified) catalysis and (**D**) CAT (from tissue lysates) catalysis. The indole (or indoline) peaks (1515 and 1605 cm^{-1}) and the broad peak spanning 3200-3500 cm^{-1} (hydroxyl structures) in CAT catalyzed polymerization products are nearly identical with peaks in the PDA standard.

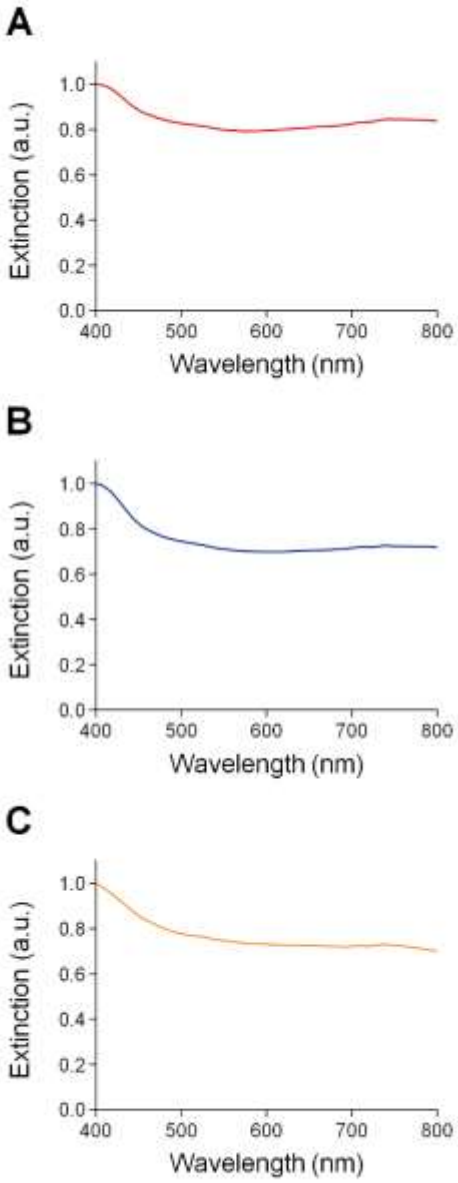

Fig. S3. Normalized extinction spectra of PDA standard and polymerization products. UV-Vis spectra of (**A**) PDA standard, (**B**) polymerization product under CAT (commercially purified) catalysis, and (**C**) polymerization product under CAT (from tissue lysates) catalysis are nearly identical, confirming the PDA formation in (**B**) and (**C**).

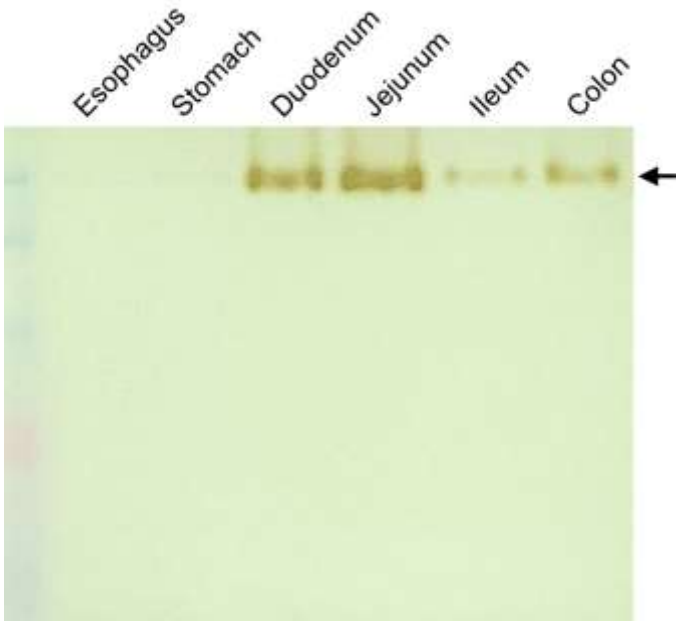

Fig. S4. Catalytic capacity analysis of tissue lysates through native gel electrophoresis. Tissue lysates from different parts of the porcine gastrointestinal tract were loaded on a non-denaturing polyacrylamide gel, electrophoresed to allow protein separation, and stained for catalytic capacity analysis. After staining by using the GSEL solution, dark-brown PDA signal can be visualized on the gel. Only one sharp band (indicated by the arrow) can be observed in each lane, supporting CAT's predicted role as the sole enzyme responsible for PDA polymerization.

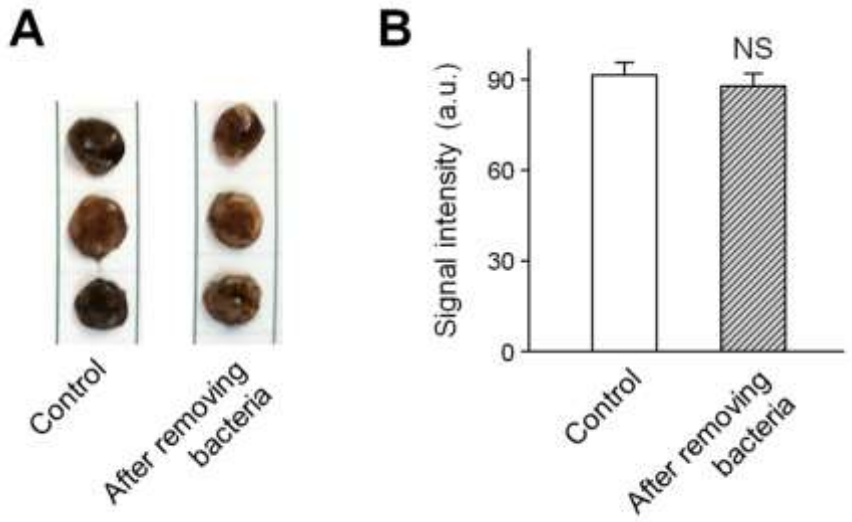

Fig. S5. Evaluation of the GSEL coating performance on the epithelium after removing bacteria present in the small intestinal mucus. (**A**) Images showing porcine tissue samples (with and without removing bacteria) after the ex vivo GSEL coating. Samples (6 mm in diameter) were collected at three random sites of PDA coated tissue. Bacteria was removed from the luminal surface of epithelium by incubation with the antibiotic-antimycotic solution and repeated washing. (**B**) Quantitative measurements of the PDA signal intensities of samples shown in (**B**). The intensity differences are not statistically significant. $P > 0.05$ by the two-tailed *t*-test. Data are reported as means ± SD over three different tissue samples.

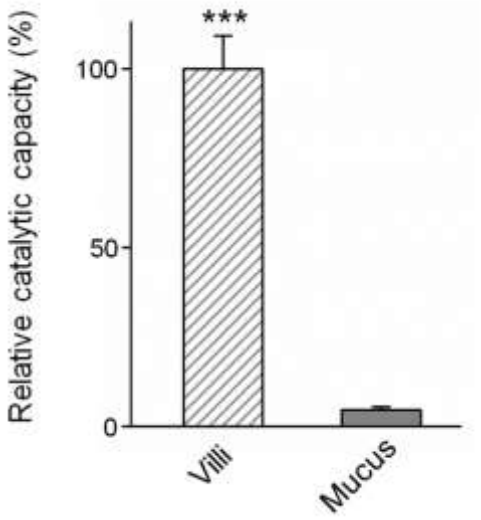

Fig. S6. Comparison of the CAT catalytic capacity between the epithelium and mucus (bacteria). The relative catalytic capacity of porcine intestinal villi (without bacteria) is significantly higher than that of bacteria in the mucus. Mucus was collected on top of the epithelium (3 cm^2), and epithelial villi was collected from the same tissue area. Samples were diluted to the same volume for measurements. The capacity differences are statistically significant. ***$P < 0.001$ by two-tailed *t*-test. Data are reported as means ± SD over three different replicates.

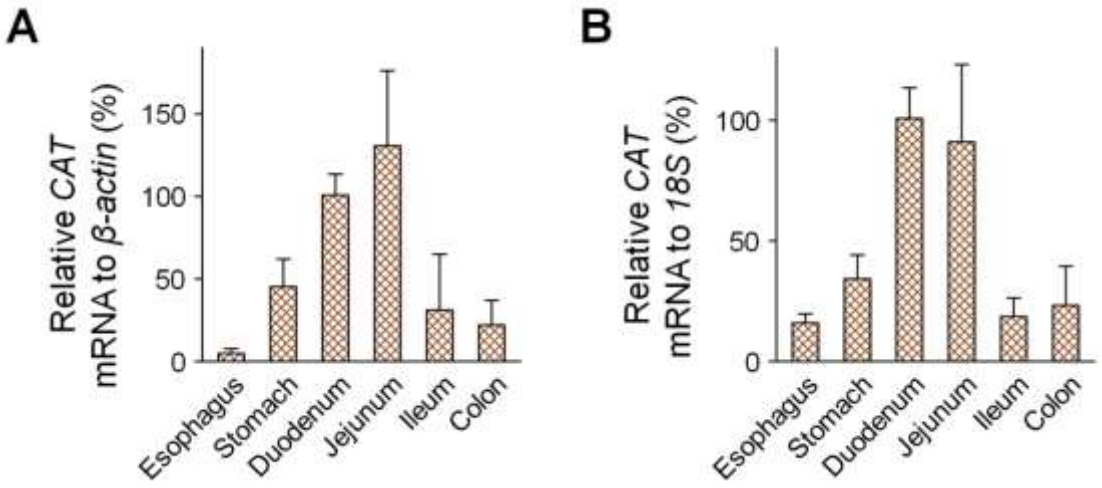

Fig. S7. Quantification of CAT mRNA in tissue using real-time PCR. Housekeeping genes, including (**A**) β-actin and (**B**) 18S, were used as controls for quantifying CAT mRNA. Tissue specimens from 4 pigs were tested. Data are reported as means ± SD over 4 animals.

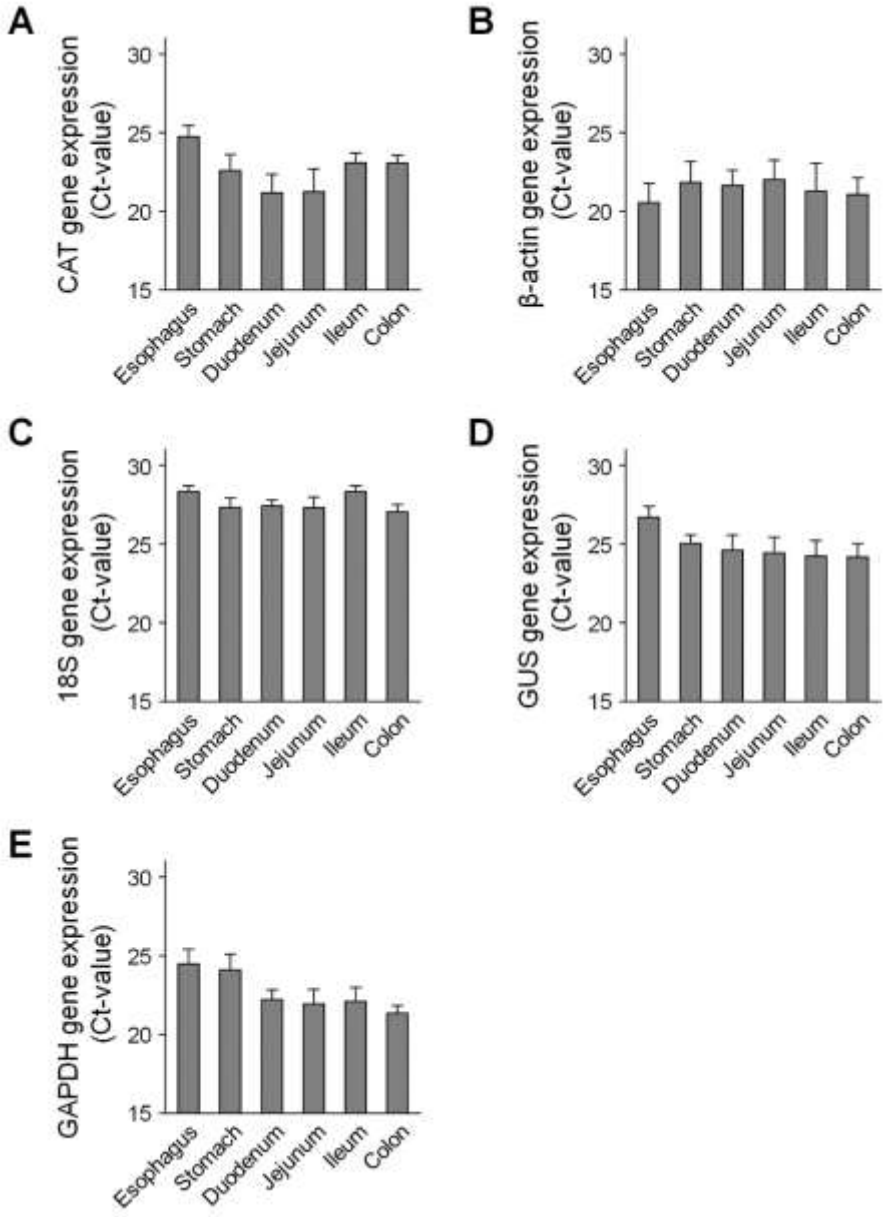

Fig. S8. C_t values of gene expression. For mRNA-level quantification, (**A**) CAT, (**B**) β-actin, (**C**) 18S, (**D**) GUS, and (**E**) GAPDH genes were included in the test. Tissue specimens from 4 pigs were tested. Data are reported as means ± SD over 4 animals.

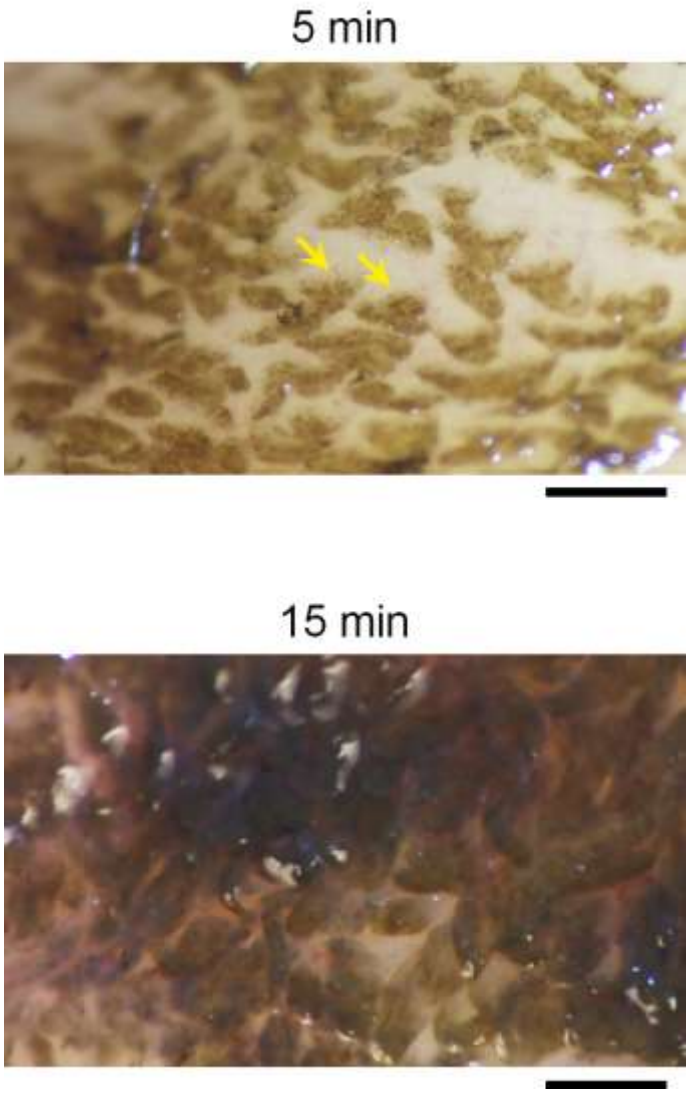

Fig. S9. Bright-field images of the PDA-coated small intestinal epithelium. Porcine small intestinal tissues were exposed to the GSEL solution ex vivo for 3 and 15 minutes, and examined under the brightfield microscopy. PDA first deposited on intestinal villus tips (indicated by yellow arrows, top panel), and then coated the whole villi, as well as surrounding area (bottom panel). Scale bars, 500 μm.

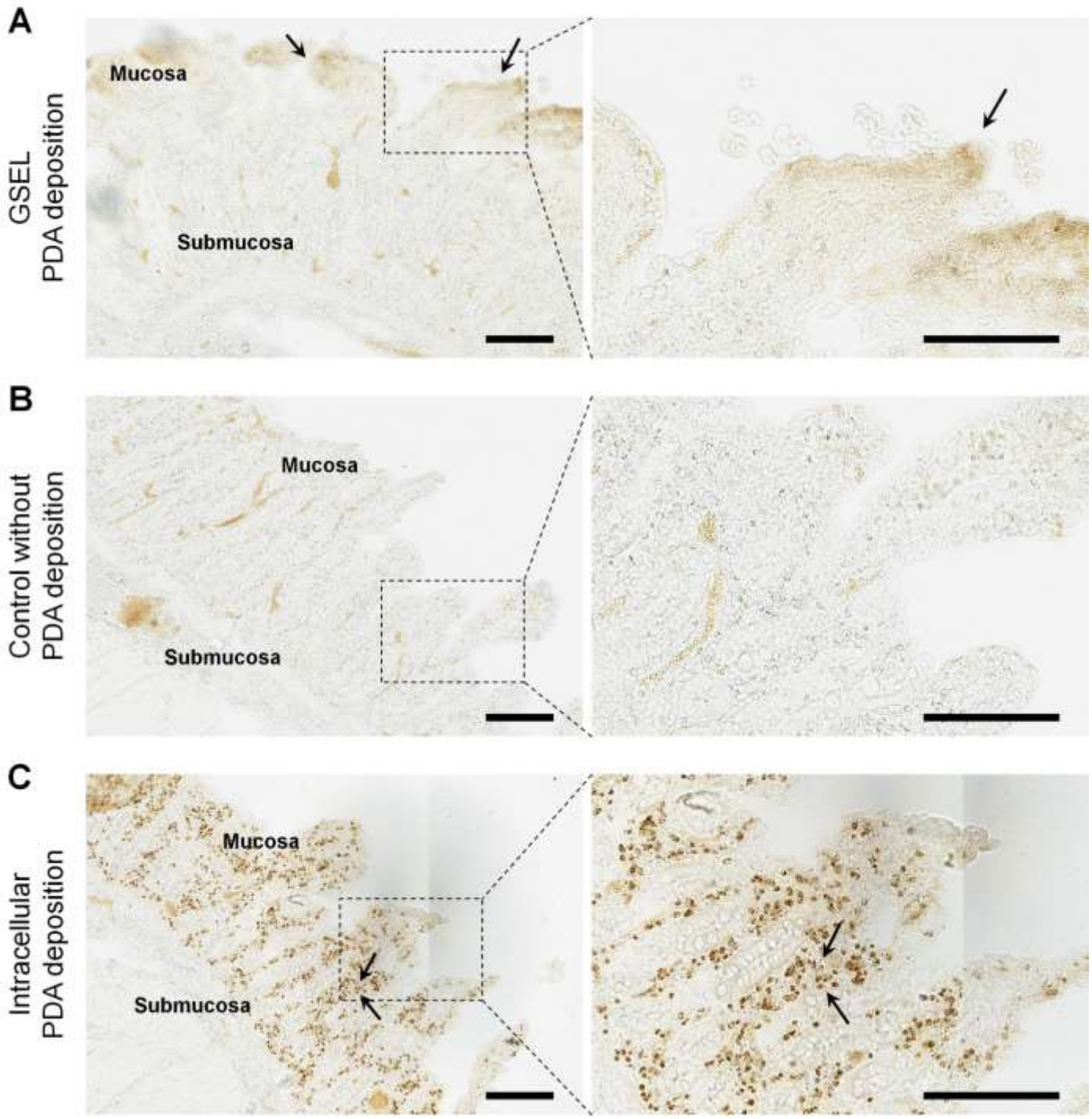

Fig. S10. Microscopic analysis of PDA epithelial deposition. (**A**) Bright-field imaging of GSEL coated porcine tissue slices. The dark-brown PDA layer only deposited on the luminal surface of the epithelial cells (indicated by arrows), but not inside cells. (**B**) Bright-field imaging of uncoated tissue slices. Light yellow background signals come from the blood vessels. (**C**) Bright-field imaging of intracellular PDA deposition on the sectioned control tissue slices, where both dopamine and hydrogen peroxide molecules can diffuse freely and instantly into the epithelial cells. Dark-brown PDA deposition (indicated by arrows) can be observed inside the epithelial cells but not on the surface of the cells, and the deposition pattern is strikingly different relative to the GSEL coated tissue slices. Scale bars, 150 μm.

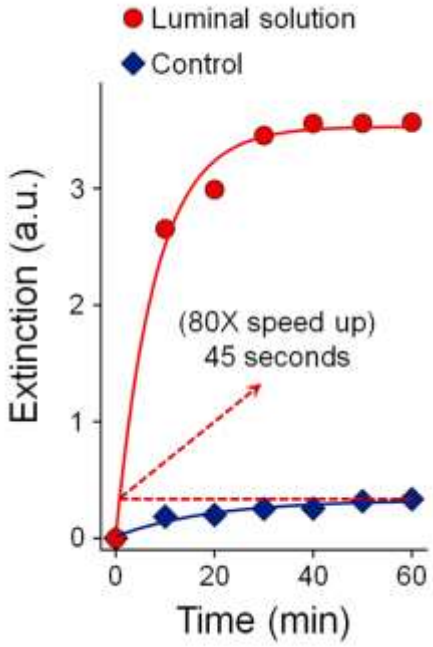

Fig. S11. PDA polymerization kinetics in the luminal solution. The PDA polymerization kinetics were evaluated in the luminal solution localized on top of porcine epithelium through ex vivo studies. Extinction was measured at 700 nm for the samples undergoing PDA polymerization. The PDA polymerization kinetics in the GSEL solution (without epithelium catalysis) were used as the control. The optical extinction produced in 45 seconds under epithelium catalysis was the same as the extinction produced in 1 hour under the control condition.

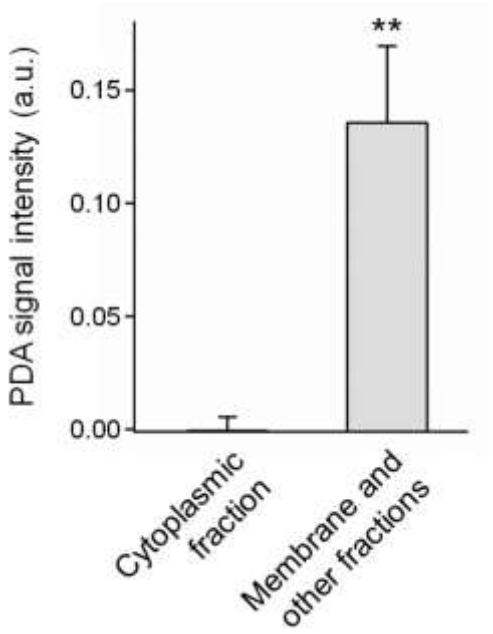

Fig. S12. Evaluation of PDA signals in different cellular fractionations. Cell fractionation was performed on GSEL coated porcine villi and PDA signals were evaluated by measuring the extinction of each cellular fraction at 700 nm. No PDA signal was detected in the cytoplasmic fraction, but PDA signal was detected in membrane and other fractions. The intensity differences are statistically significant. $^{**}P < 0.01$ by the two-tailed *t*-test. Data are reported as means ± SD over three replicates.

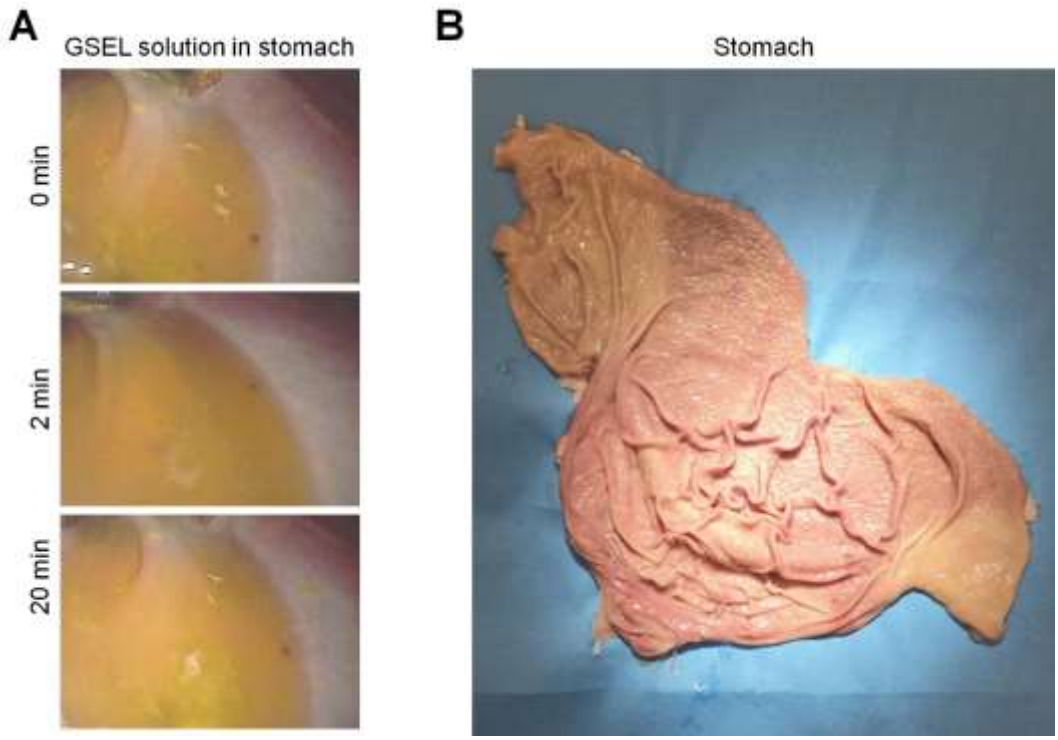

Fig. S13. Evaluation of in vivo GSEL coating performance in the stomach. (**A**) Endoscopic images revealed that no dark-brown PDA was visualized in the porcine stomach. The GSEL solution in the stomach remains clear over 20 minutes. (**B**) Image of the isolated stomach from the animal in (**A**) confirming no PDA coating on the epithelial surface.

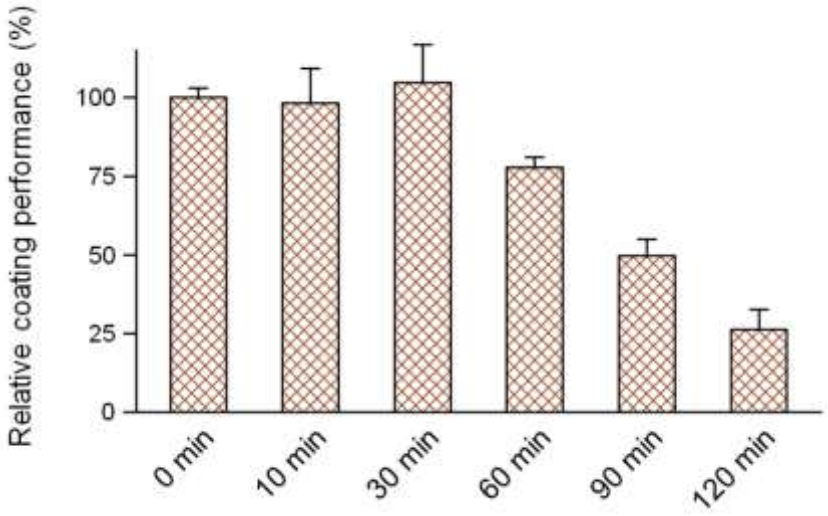

Fig. S14. Evaluation of the stability of the GSEL solution in the stomach. To evaluate the stability, the GSEL solution was in vivo administrated to the pig (non-crushing clamp was applied at the pylorus), retrieved from the stomach at different time points, and characterized through ex vivo coating studies. The relative coating performance shows that the retrieved solutions (from 10-30 minutes) showed consistent coating performance, and the relative coating efficiency drops only 30% after 60 minutes, demonstrating that both dopamine and hydrogen peroxide in the GSEL solution were not significantly absorbed or consumed in the stomach. Data are reported as means ± SD over three replicates.

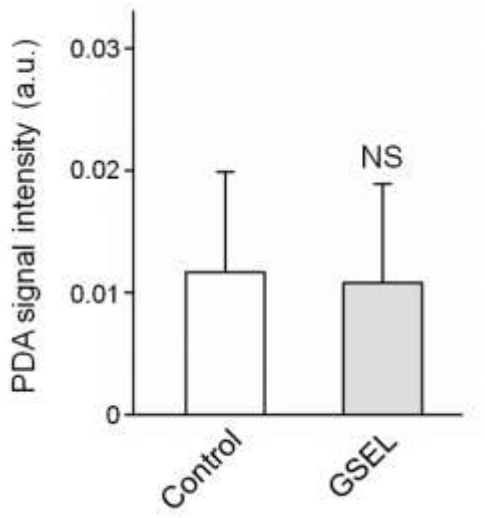

Fig. S15. Evaluation of the PDA signal in the submucosa. No detectable increase of PDA signal was observed in the porcine submucosa after the in vivo GSEL coating. Epithelium tissues (without coating) were used as controls. The signal differences are not statistically significant. $P > 0.05$ by the two-tailed *t*-test. Data are reported as means ± SD over three replicates.

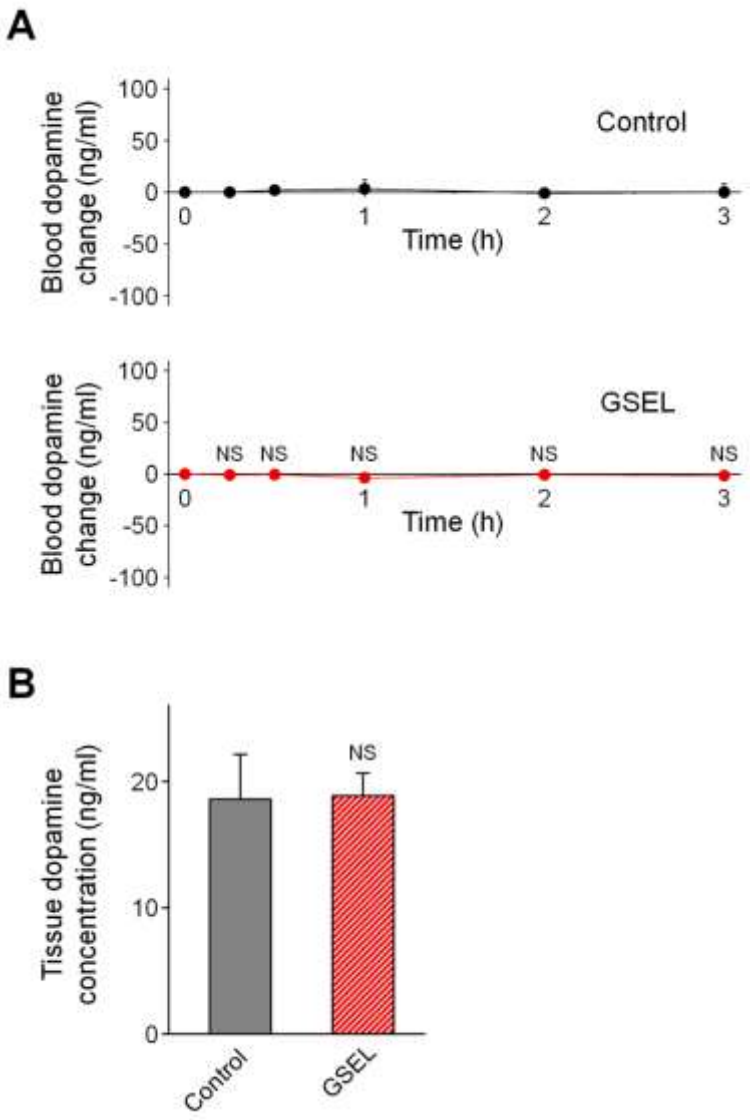

Fig. S16. Evaluation of the dopamine concentration in the blood and submucosa through liquid chromatography–tandem mass spectroscopy. (**A**) No obvious change of dopamine concentration was observed in the porcine blood after in vivo administration of the GSEL solution. $P > 0.05$, two sample *t* test comparing GSEL and control groups (without GSEL solution) at matching time points. Data are reported as means ± SD over three animals. (**B**) No detectable increase of dopamine concentration was observed in the porcine submucosa after in vivo administration of the GSEL solution (after 3 hours). The concentration differences are not statistically significant. $P > 0.05$ by the two-tailed *t*-test. Data are reported as means ± SD over three replicates.

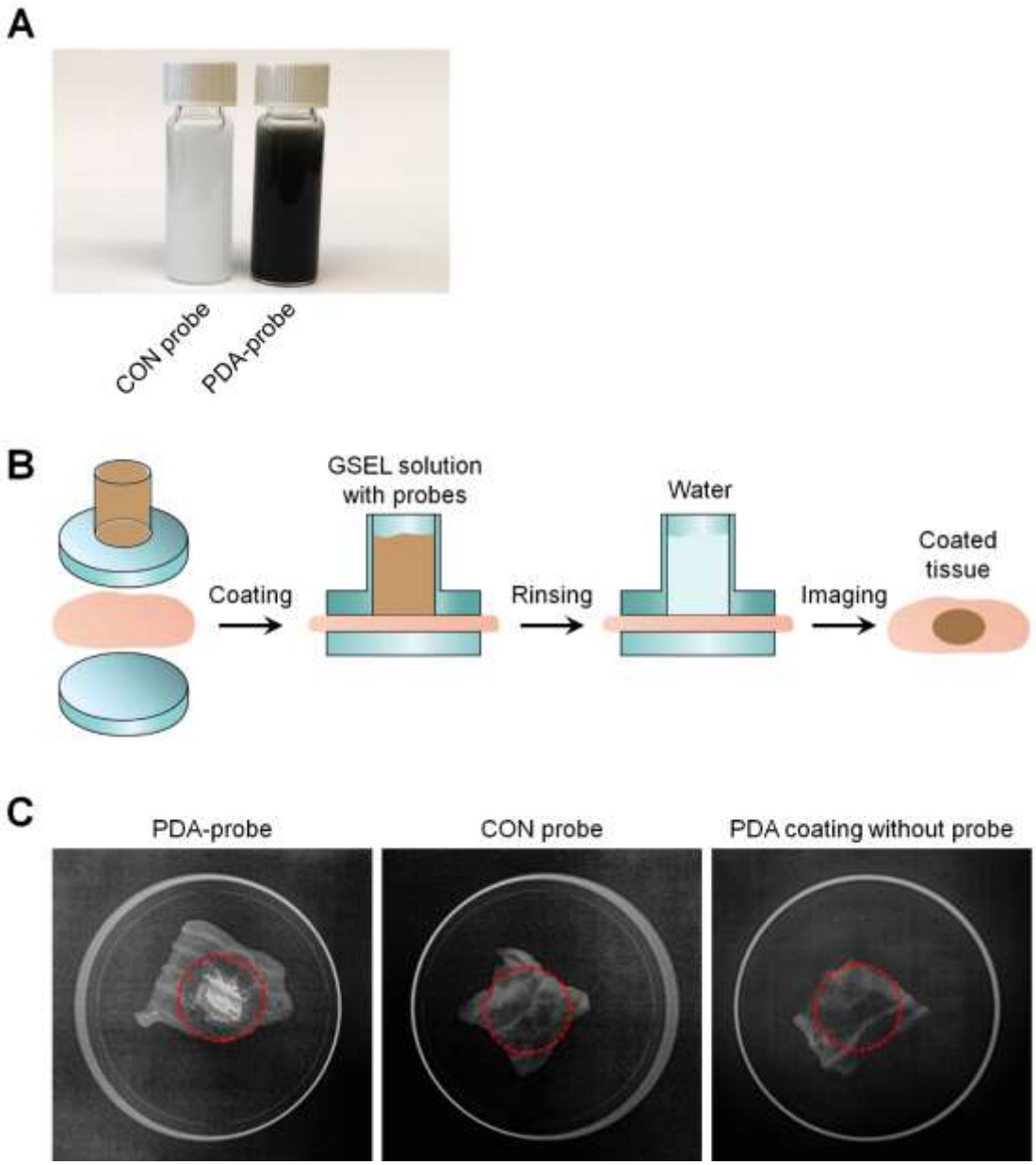

Fig. S17. Evaluation of ex vivo PDA probe tissue-coating performance through x-ray imaging. (**A**) Images showing the conventional (CON) probe solution and PDA-probe solution. The PDA probe was prepared by encapsulating the conventional probe with a thin layer PDA. The dark-brown color of the PDA-probe solution comes from chromogenic PDA on the probe surface. (**B**) Schematic illustration of the ex vivo tissue-coating process. The porcine small intestine was placed in the Franz Cell, and the GSEL solution (with or without probes) was added into the chamber. After the coating, the coated tissue was rinsed by the water and imaged by the X-ray system. (**C**) X-ray images of porcine tissues coated by using the GSEL solution with PDA-probes (left panel), conventional (CON) probes (middle panel), and the GSEL solution without probes (right panel). Strong X-ray signals were only observed in the coated area (indicated by red circles) of the PDA-probe coated tissue. No obvious X-ray signal was detected in controls where conventional probes or PDA alone were applied for coating.

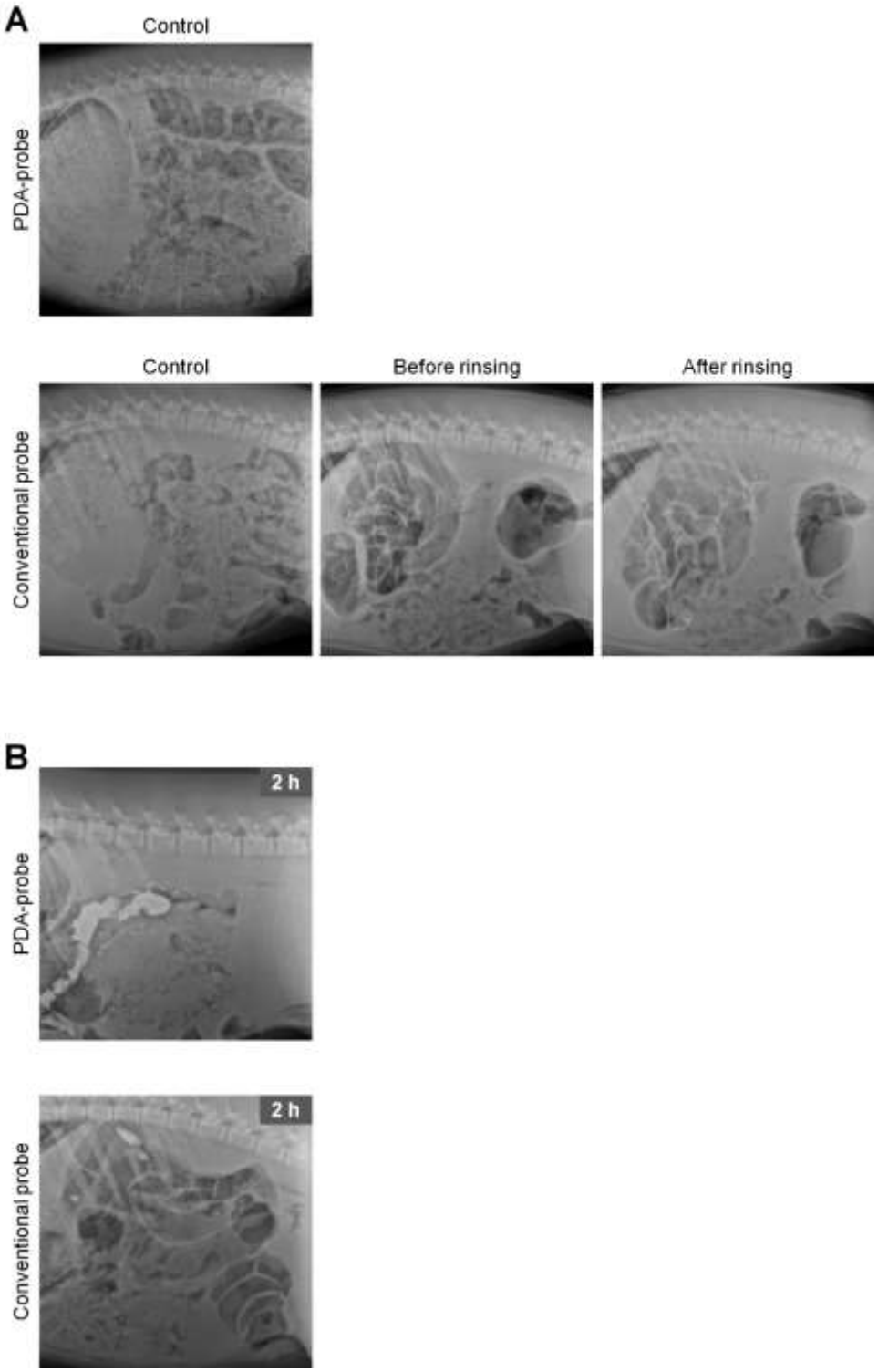

Fig. S18. In vivo x-ray imaging of the intestinal retention of the PDA coating layer. (**A**) X-ray images revealing the PDA coating stability. Healthy pigs were orally administered the PDA probe suspended GSEL solution (top panels) and conventional probes (bottom panels) separately, and imaged by the X-ray system. The solution was directly administered to the small intestine through a catheter under endoscopic visual guidance. The same pigs without administrating probes were imaged and used as controls. Water was used for rinsing the imaging area to test the PDA coating stability. (**B**) X-ray images revealing the intestinal retention of PDA over time. A series of X-ray images were periodically taken in the same location at 2, 6, and 24 hours. Animals consistently consumed a liquid diet during imaging, mimicking realistic conditions and testing the stability of the PDA coating in the presence of food.

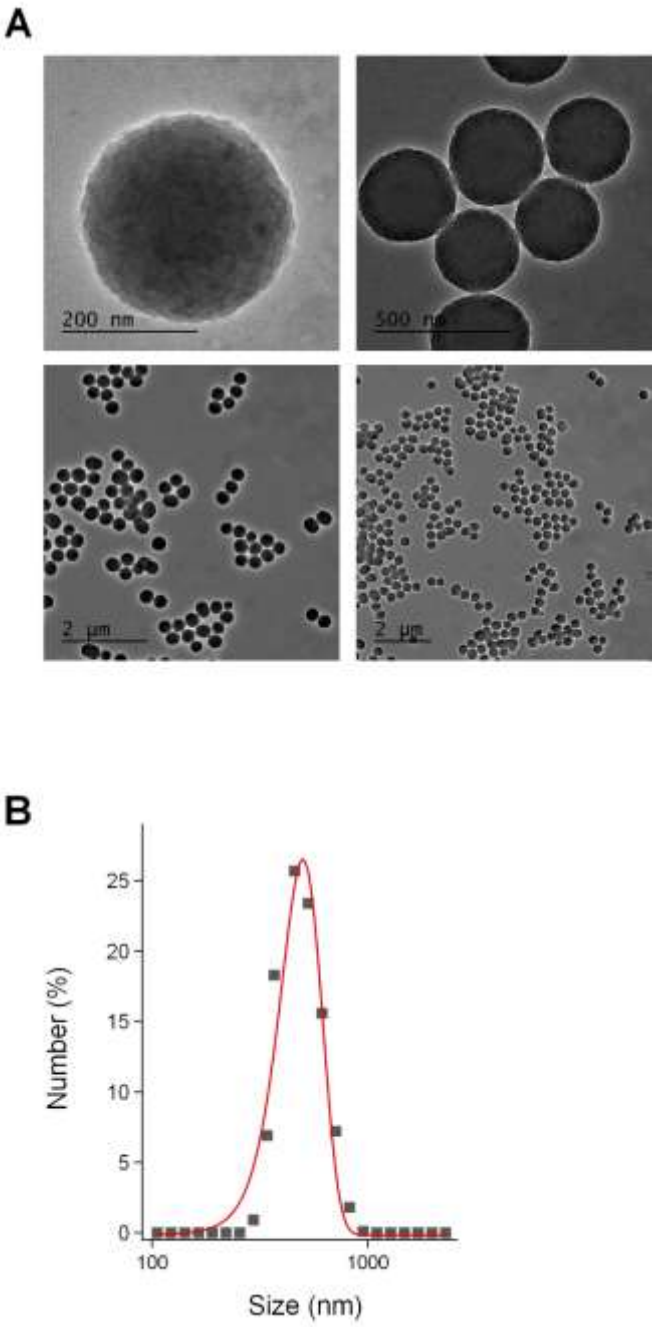

Fig. S19. Characterization of nano–cross-linkers. (**A**) TEM images with different magnifications showing uniform PDA nano-crosslinkers. (**B**) Dynamic light scattering (DLS) analysis showing nano-crosslinkers' hydrodynamic size of 527 nm.

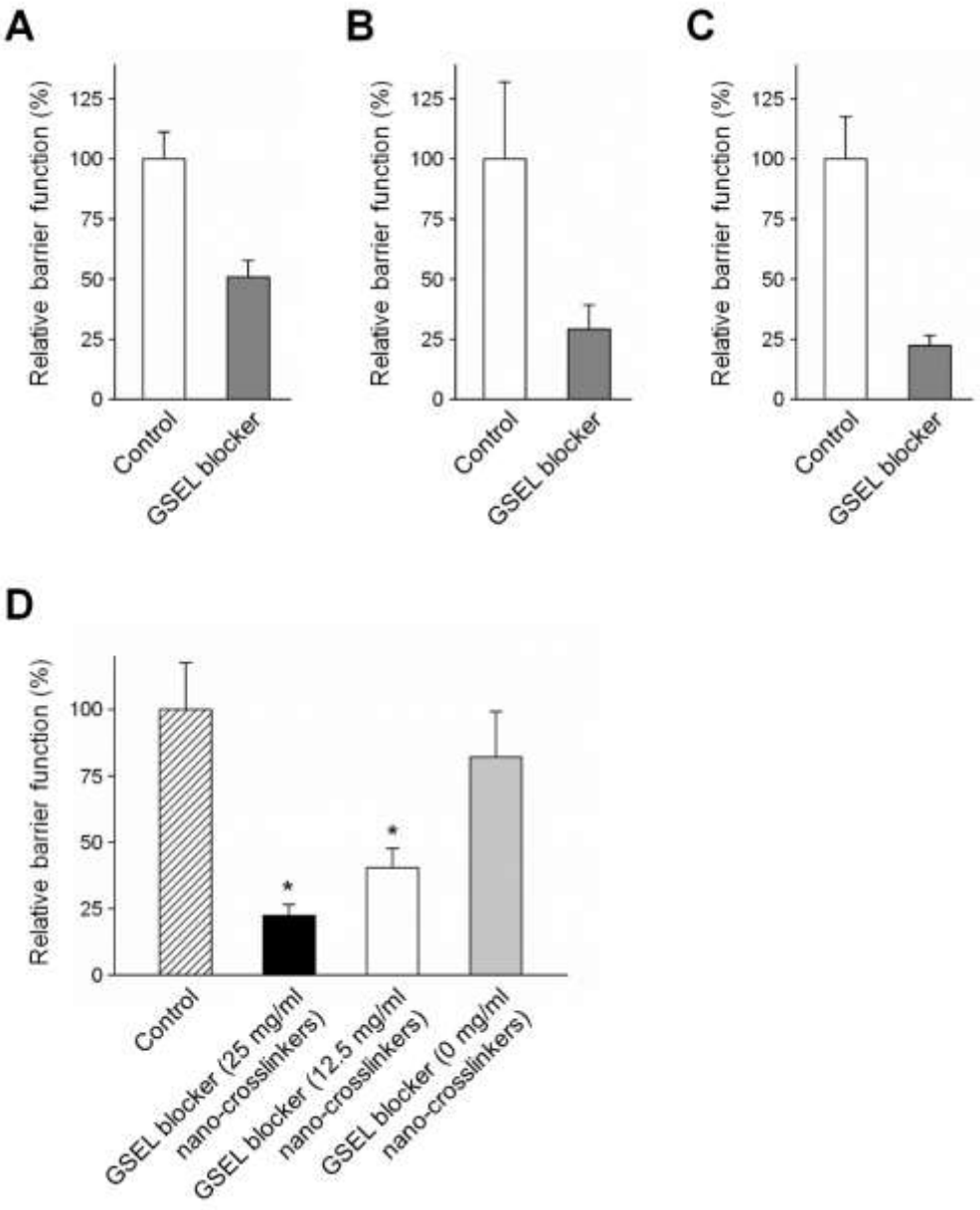

Fig. S20. Evaluation of blocking efficiency of the GSEL coating layer through ex vivo studies. (**A-C**) Relative barrier functions (tissue-penetration) of the GSEL coating layer against (**A**) Ca^{2+}, (**B**) glutamic acid, and (**C**) glucose. All three nutrients showed significantly reduced tissue-penetration, with the three separate experiments showing GSEL barrier blocking ~49% of Ca^{2+}, ~71% of glutamic acid, and ~78% of glucose. (**D**) Relative barrier functions (glucose tissue-penetration) of the GSEL coating layer (with different crosslinking densities). Porcine small intestinal tissues (without coating) were used as controls. *P < 0.05 (versus control), one-way analysis of variance (ANOVA) and post hoc Bonferroni. Data are reported as means ± SD over three replicates.

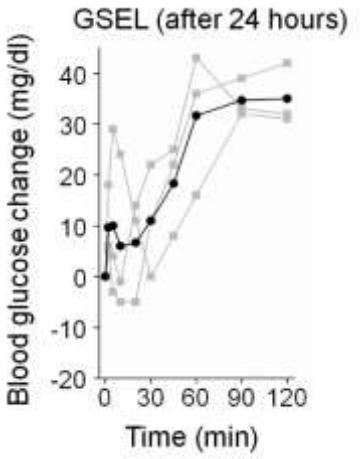

Fig. S21. Evaluation of glucose absorption restoring of GSEL animals. An oral glucose tolerance test was performed 24 hours after pigs received GSEL coating. Pigs with the GSEL coating recovered normal glucose absorption after 24 hours, demonstrating that the GSEL coating layer is transient. Data was averaged between animals (each animal represented by a grey line) in each group (shown by the black line).

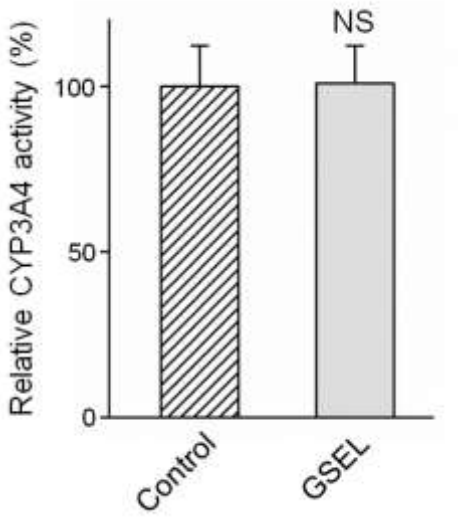

Fig. S22. Evaluation of the CYP450 activity of epithelium with and without the PDA coating layer. The CYP450 activity of porcine tissues was ex vivo evaluated. Epithelium tissues (without coating) were used as controls. The activity differences are not statistically significant. $P > 0.05$ by the two-tailed *t*-test. Data are reported as means ± SD over five replicates.

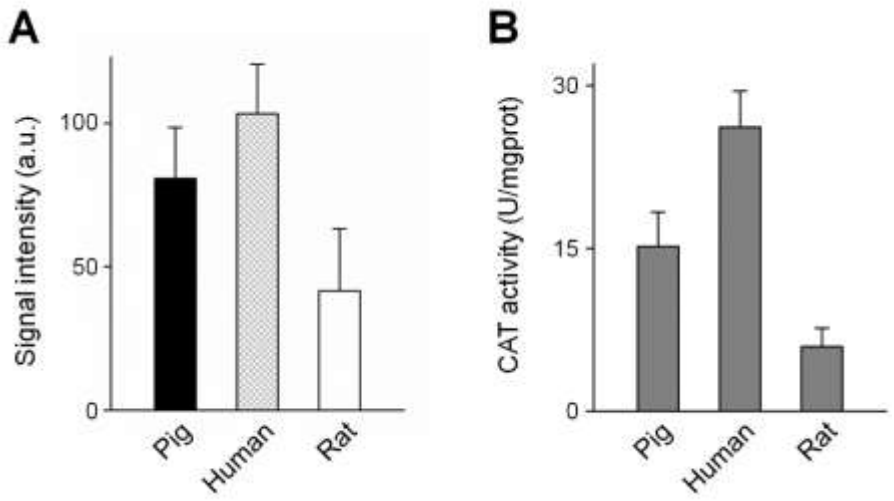

Fig. S23. Evaluation of the GSEL coating performance across different animal species. (**A**) Quantitative ex vivo evaluation of the PDA coating density on small intestines from pig, human, and rat. PDA signal intensities were measured after applying the GSEL coating, representing the PDA coating density. Data are reported as means ± SD over three replicates. (**B**) Quantification of CAT expression by measuring the CAT activity in small intestines from pig, human, and rat. Tissue specimens were collected from same animals in (**A**). Data are reported as means ± SD over three replicates.

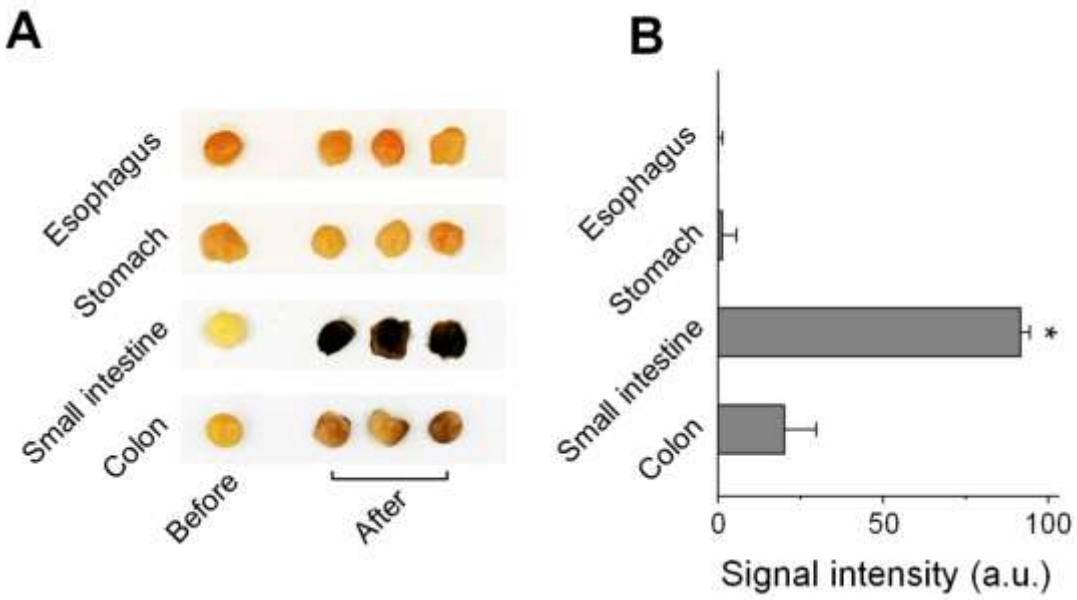

Fig. S24. GSEL coating pattern in the human GI tract. (**A**) Images showing human tissue samples from different parts of the GI tract before and after applying the GSEL coating ex vivo. Samples (6 mm in diameter) were collected at three random sites of PDA coated tissue. (**B**) Quantitative measurements of the PDA signal intensities of samples shown in (**B**). The intensity differences between the small intestine and other tissues are statistically significant. *P < 0.05, one-way analysis of variance (ANOVA) and post hoc Bonferroni. Data are reported as means ± SD over three different tissue samples.

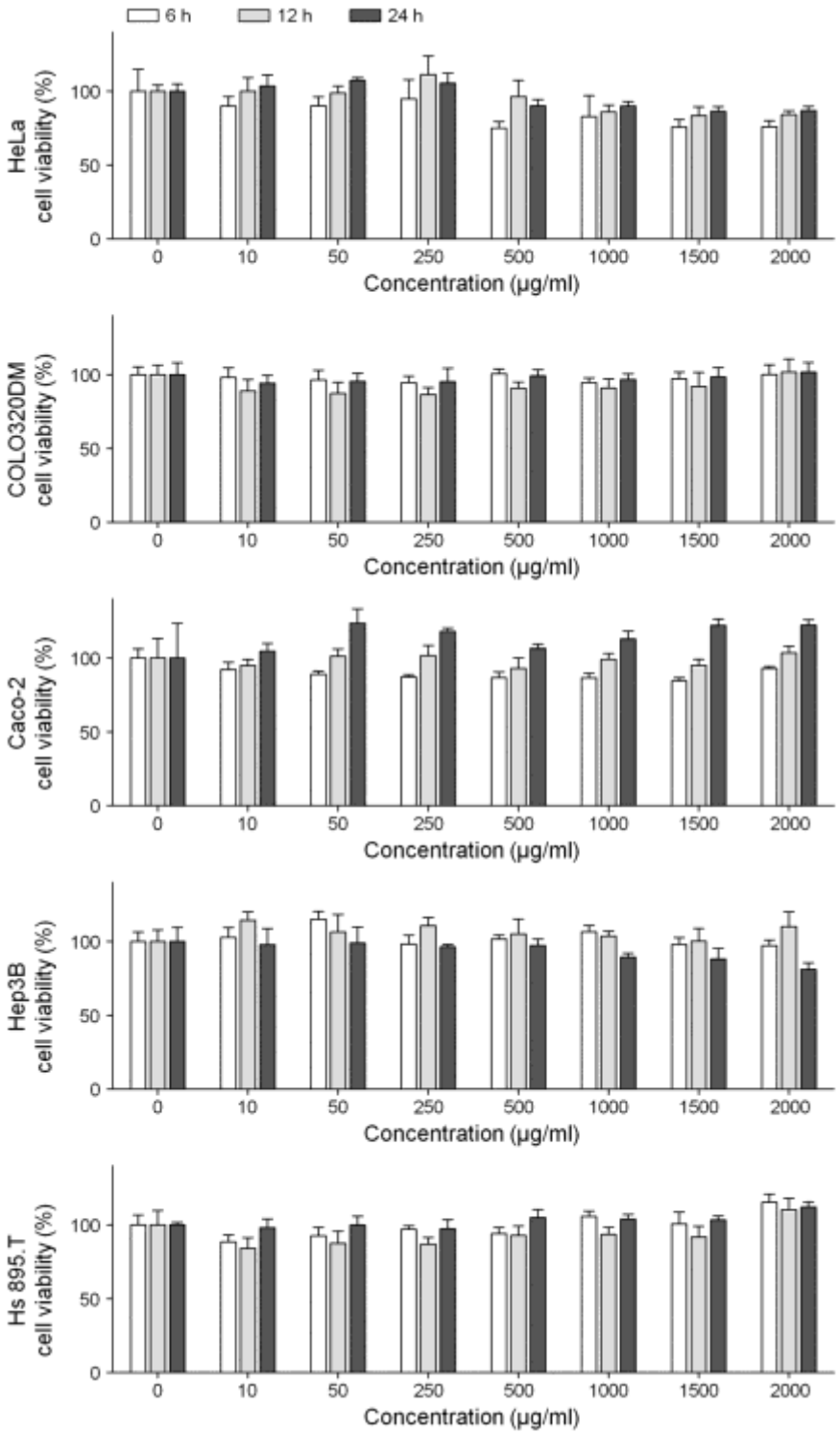

Fig. S25. Dose-dependent cytotoxicity of PDA in HeLa, COLO320DM, Caco-2, Hep3B, and HS 895.T cells. Cells were treated with PDA at various concentrations, and cytotoxicity was analyzed at different time points. PDA is of low toxicity (>80% viability) in the concentration range of 0-2000 µg/ml for all cell lines after 24 hour PDA exposure.

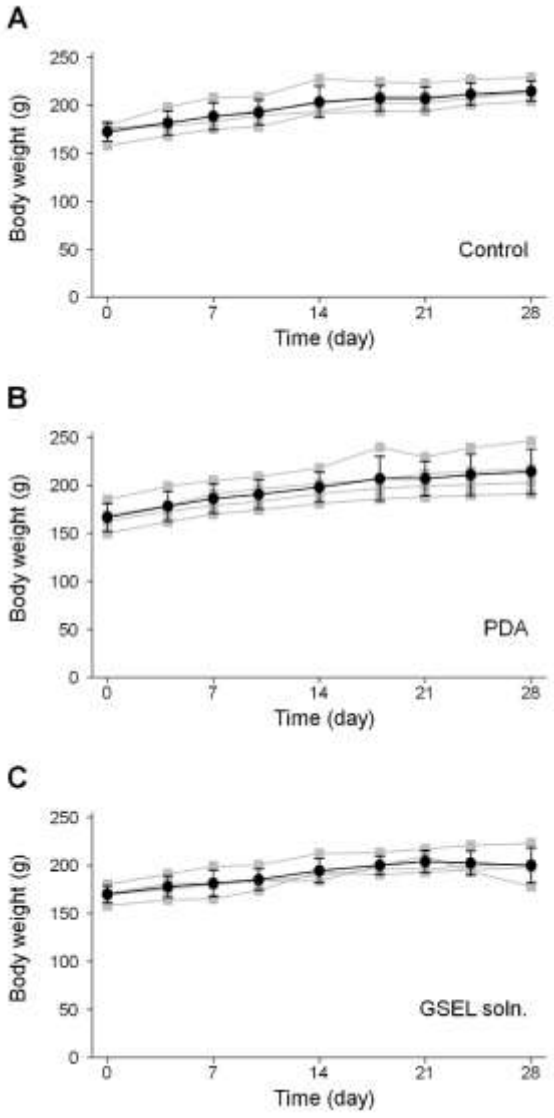

Fig. S26. Body weight changes of rats during the 28-day oral toxicity evaluation. Rats were exposed to (**A**) water (control), (**B**) as-prepared PDA, and (**C**) the GSEL solution separately over a period of 4 weeks. No significant differences in body weights were observed between rats exposed to the GSEL solution, PDA and water. Data was averaged between animals (each animal represented by a grey line) in each group (shown by the black line). Data are reported as means ± SD over four animals.

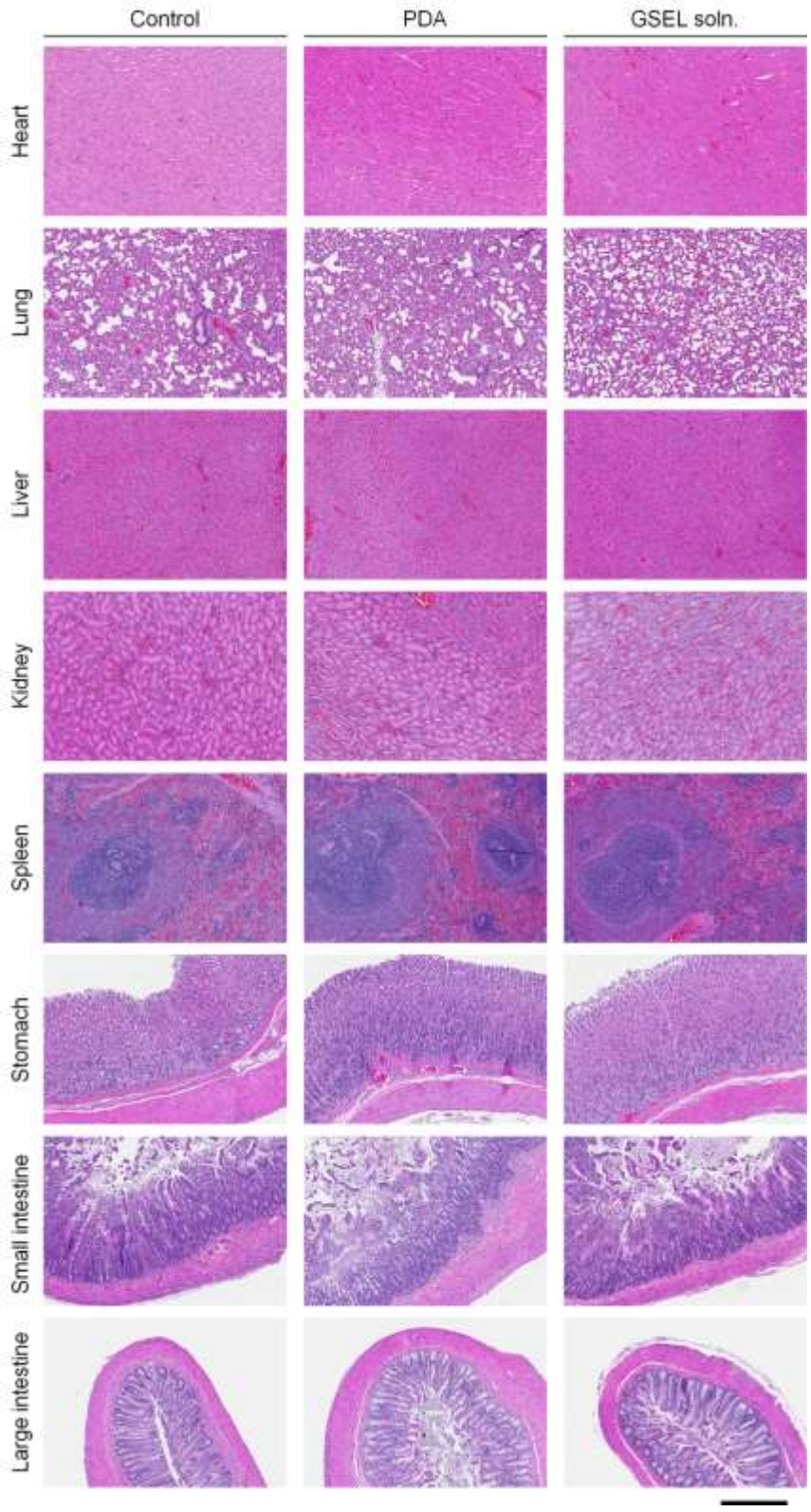

Fig. S27. Histology of the major organs collected from rats after 28-day oral toxicity evaluation. Tissues were collected from rats exposed to water (control), as-prepared PDA, and the GSEL solution separately. Scale bar, 300 μm.

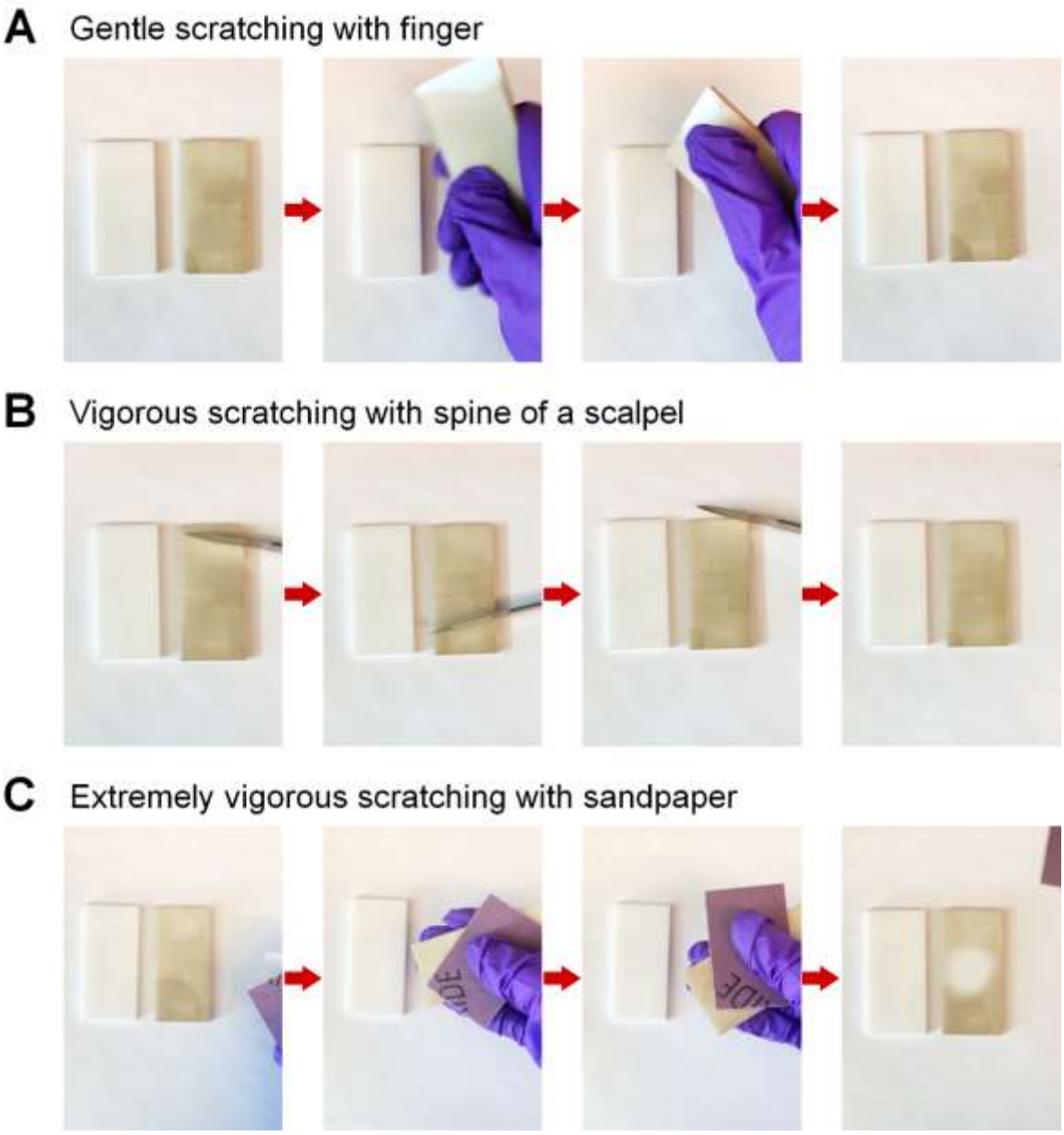

Fig. S28. Stability of the surface-based PDA coating. PDA coating was applied on the surface of impermeable polycarbonate substrate. The white color polycarbonate (left) turned into a dark-brown color after the PDA coating (right). The stability of the PDA coating was evaluated in a series of physical conditions (**A-C**). No obvious PDA signal reduction was observed under both gentle and vigorous scratching, and the PDA coating was only removed under extremely vigorous scratching with sandpaper. These results demonstrated that the stability of surface-based PDA coating is due to strong surface-based adhesion, rather than penetration into the substrate surface.

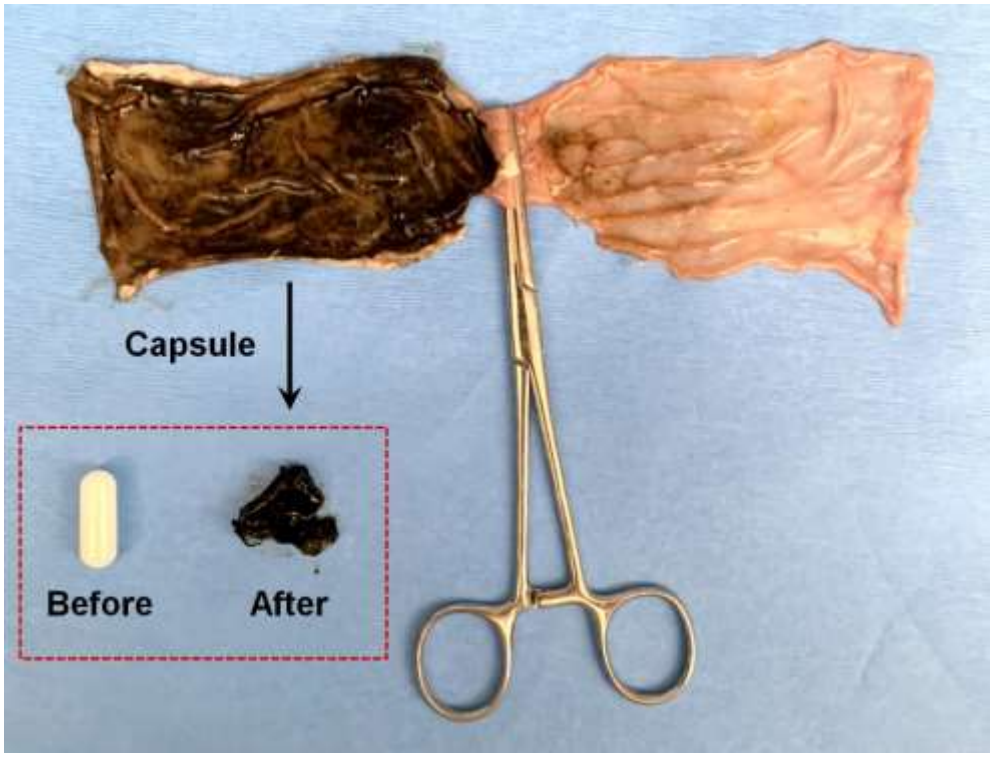

Fig. S29. Translation of the GSEL platform into capsules. Isolated porcine small intestinal tissue from the in vivo test with PDA coating before but not after the clamp site, demonstrating the coating performance of GSEL capsules. Capsules did not pass down to the lower small intestine due to the small intestinal ligation. After releasing GSEL ingredients, capsules collapsed, dissolved and broke into smaller pieces.

Table S1. Hematological measurements of blood from rats after 28-day oral toxicity evaluation. Blood samples were collected from rats exposed to water (control), as-prepared PDA, and the GSEL solution. No significant differences in the hematological parameters were observed between rats (four replicates) exposed to the GSEL solution, PDA and water.

Hematological results (mean ± s.d.)

	Control	PDA	GSEL soln.
WBC	10.52 ± 2.75	7.35 ± 1.50	10.29 ± 4.01
NEU	21.71 ± 4.72	26.70 ± 3.65	21.08 ± 2.38
LYM	72.75 ± 5.24	67.71 ± 5.34	74.06 ± 3.58
MON	4.89 ± 0.73	5.06 ± 2.25	4.11 ± 1.42
EOS	0.50 ± 0.19	0.38 ± 0.16	0.66 ± 0.50
BAS	0.15 ± 0.19	0.15 ± 0.03	0.09 ± 0.06
RBC	7.46 ± 0.22	7.30 ± 0.43	7.25 ± 0.13
HB	16.75 ± 0.91	16.08 ± 1.07	15.73 ± 0.30
HCT	43.00 ± 1.61	41.30 ± 2.52	40.65 ± 0.78
MCV	57.63 ± 1.93	56.60 ± 0.14	56.08 ± 1.99
MCH	22.45 ± 0.91	22.00 ± 0.24	21.70 ± 0.45
MCHC	38.95 ± 0.76	38.93 ± 0.33	38.70 ± 0.88
RDW	14.60 ± 0.20	14.90 ± 0.20	14.85 ± 0.44
MPV	6.75 ± 0.26	7.33 ± 0.64	7.00 ± 0.45

Note. *WBC* (K/μL), white blood cells; *NEU* (%), neutrophils; *LYM* (%), lymphocytes; *MON* (%), monocytes; *EOS* (%), eosinophils; *BAS* (%), basophils; *RBC* (M/μL), red blood cells; *HB* (g/dL), hemoglobin; *HCT*(%), hematocrits; *MCV* (fl), mean corpuscular volume; *MCH* (pg), mean corpuscular hemoglobin; *MCHC* (g/dL), mean corpuscular hemoglobin concentration; *RDW* (%), red cell distribution width; *MPV* (fl), mean platelet volume.

Table S2. Blood biochemistry tests of blood from rats after 28-day oral toxicity evaluation. Blood samples were collected from rats exposed to water (control), as-prepared PDA, and the GSEL solution. No significant differences in the blood biochemistry parameters were observed between rats (four replicates) exposed to the GSEL solution, PDA and water.

Blood biochemistry results (mean ± s.d.)

	Control	PDA	GSEL soln.
AST	73.25 ± 2.63	87.25 ± 10.34	79.25 ± 9.74
GGT	0.50 ± 0.58	1.00 ± 0.00	0.25 ± 0.50
ALB	3.23 ± 0.17	3.55 ± 0.10	3.43 ± 0.19
TBIL	0.20 ± 0.00	0.25 ± 0.06	0.20 ± 0.00
CRE	0.68 ± 0.15	0.83 ± 0.30	0.70 ± 0.08
CHO	57.50 ± 9.75	68.25 ± 9.71	61.50 ± 7.85
GLU	223.50 ± 53.97	198.00 ± 18.02	212.00 ± 49.96
P	7.73 ± 0.67	8.28 ± 1.38	7.83 ± 0.33
Cl	100.25 ± 1.71	100.25 ± 1.71	99.75± 2.22
K	8.38 ± 1.16	9.60 ± 2.64	8.23 ± 0.49
Na	138.00 ± 2.16	138.25 ± 2.22	138.50 ± 3.11

Note. *AST* (IU/L), aspartate aminotransferase; *GGT* (IU/L), gamma glutamyl transferase; *ALB* (g/dL), albumin; *TBIL* (mg/dL), total bilirubin; *CRE* (mg/dL), creatinine; *CHO* (mg/dL), cholesterol; *GLU* (mg/dL), glucose; *P* (mg/dL), phosphorus; *Cl* (mEq/L), chloride; *K* (mEq/L), potassium; *Na* (mEq/L), sodium.

Movie S1. Human tissue-coating stability test I. No obvious PDA signal reduction was observed from PDA coated human small intestine after vigorous scratching the tissue using the spine of a scalpel.

Movie S2. Human tissue-coating stability test II. No obvious PDA signal reduction was observed from PDA coated human small intestine after vigorous stirring the tissue in water.